

A 40TH DEGREE AND ORDER GRAVITATIONAL FIELD MODEL FOR MARS; *M.T. Zuber¹, D.E. Smith¹, F.J. Lerch¹, R.S. Nerem¹, G.B. Patel², and S.K. Fricke³*, ¹Laboratory for Terrestrial Physics, NASA/Goddard Space Flight Center, Greenbelt, MD 20771; ²ST Systems Corporation, Lanham, MD 20706; ³RMS Technologies, Inc., Lanham, MD 20706.

Understanding of the origin and evolution of major physiographic features on Mars, such as the hemispheric dichotomy and Tharsis rise, will require improved resolution of that planet's gravitational and topographic fields. The highest resolution gravity model for Mars published to date [1] was derived from Doppler tracking data from the Mariner 9 and Viking 1 and 2 spacecraft, and is of 18th degree and order. That field has a maximum spatial resolution of approximately 600 km, which is comparable to that of the best current topographic model [2]. The resolution of previous gravity models was limited not by data density, but rather by the computational resources available at the time. Because this restriction is no longer a limitation, we have re-analyzed the Viking and Mariner datasets and have derived a gravitational field complete to 40th degree and order with a corresponding maximum spatial resolution of 300 km where the data permit.

Derivation of the field was based on analysis of 235 orbital arcs consisting of 1200 days of S-band Doppler tracking data from the Mariner 9 and Viking 1 and 2 spacecraft, collected by the Deep Space Network from 1971-1978. The data were processed using the GEODYN/SOLVE orbit determination programs. These programs, which have previously been used in the determination of a series of standard Earth gravitational models (the "GEM" models [cf. 3]), have recently been adapted for analysis of planetary tracking data [4].

The Martian gravitational potential at spacecraft altitude was represented in spherical harmonic form [5]

$$V_M(\vec{r}) = \frac{GM_M}{r} \sum_{l=0}^N \sum_{m=0}^l \left(\frac{r_M}{r} \right)^l P_{lm}(\sin\phi) [C_{lm} \cos m\lambda + S_{lm} \sin m\lambda] \quad (1)$$

where \vec{r} is the position vector of the spacecraft in areocentric coordinates, r is the radial distance from the center of mass of Mars to the spacecraft, ϕ and λ are the areocentric latitude and longitude of the spacecraft, r_M is the mean radius of the reference ellipsoid of Mars, G is the gravitational constant, M_M is the mass of Mars, P_{lm} are the normalized associated Legendre functions of degree l and order m , C_{lm} and S_{lm} are the normalized spherical harmonic coefficients which were estimated from the tracking observations to define the gravitational model, and N is the maximum degree representing the size (or resolution) of the field. The gravitational force due to Mars which acts on the spacecraft corresponds to the gradient of the potential, V_M . In our analysis, the origin of the field was taken to be the center of mass of Mars, which required that $C_{00}=1$ and $S_{00}=C_{10}=C_{11}=S_{11}=0$.

To determine the field, orbits were computed for each arc by estimating from the tracking data the initial position and velocity of the spacecraft, along with the atmospheric drag, solar radiation pressure, and Doppler tracking biases. After the arc solutions were iterated to convergence, information equations were created for each arc by evaluating the partial derivatives of the observations with respect to the arc parameters and gravity coefficients along each arc. The gravitational model was then found by adding together the information equations for each arc and solving the resulting linear system. The dominant error sources in the model are the uncertainties in the spacecraft orbits, which are affected by the tracking coverage as well as the assumed models of atmospheric drag and solar radiation pressure, and perturbations caused by spacecraft angular momentum desaturations. Details of the treatment of these parameters are discussed in [4]. As in previous analyses [e.g. 1], we imposed *a priori* constraints on the model based upon Kaula's Rule [5] rescaled to Mars, which causes poorly observed (usually high degree and order) coefficients to tend toward zero, but has little effect on coefficients that are well sensed by the tracking data [3,6].

Error analyses based on the observation data demonstrate that the new field is characterized by a significantly better rms orbital accuracy ($=0.212 \text{ cm s}^{-1}$) than previous models ([1]= 0.535 cm s^{-1}). In

addition, the field shows a greater resolution of identifiable geological structures. Free air gravity anomalies calculated from the most recent iteration of the model, MGM-515, are plotted in Figure 1. As for previous models, the gravity anomalies correlate well with principal features of Martian topography, indicating either that topography is only partially compensated, or that deep-seated mantle processes are responsible for both the topography and gravity [7]. For the current model, gravity anomalies associated with essentially all major features, including volcanic shields, impact basins and the Valles Marineris, show considerably higher magnitudes than in previous models. A higher dynamic range of power (2100 m vs. 1950 m for [1]) is also observed in the geoid representation of the field. Figure 1 also shows a possible trend along the hemispheric dichotomy of Mars in the longitude range $120^{\circ} < \lambda < 240^{\circ}$. Free air anomalies across the dichotomy boundary would be inconsistent with a simple model of isostatic compensation due to a change in crustal thickness across the boundary, such as suggested by [8]. However, detailed modeling of individual arcs which cross the boundary in areas spatially removed from the influence of Tharsis and Elysium will be required to more accurately resolve the nature of the gravity signature of this feature.

References: [1] Balmino, G., B. Moynot, and N. Vales, *J. Geophys. Res.*, 87, 9735-9746, 1982. [2] Bills, B.G., and A.J. Ferrari, *J. Geophys. Res.*, 83, 3497-3508, 1978. [3] Marsh, J.G., et al., *J. Geophys. Res.*, 93, 6169-6125, 1988. [4] Smith, D.E., F.J. Lerch, J.C. Chan, D.S. Chinn, H.B. Iz, A. Mallama, and G.B. Patel, *J. Geophys. Res.*, 95, 14115-14167, 1990. [5] Kaula, W.M., *Theory of Satellite Geodesy*, 124 pp., Blaisdell, Waltham, 1966. [6] Lerch, F.J., et al., *NASA TM 100713*, 1988. [7] Phillips, R.J., and K. Lambeck, *Rev. Geophys.*, 18, 27-76, 1980. [8] Phillips, R.J., *EOS Trans. Am. Geophys. Un.*, 16, 389, 1988.

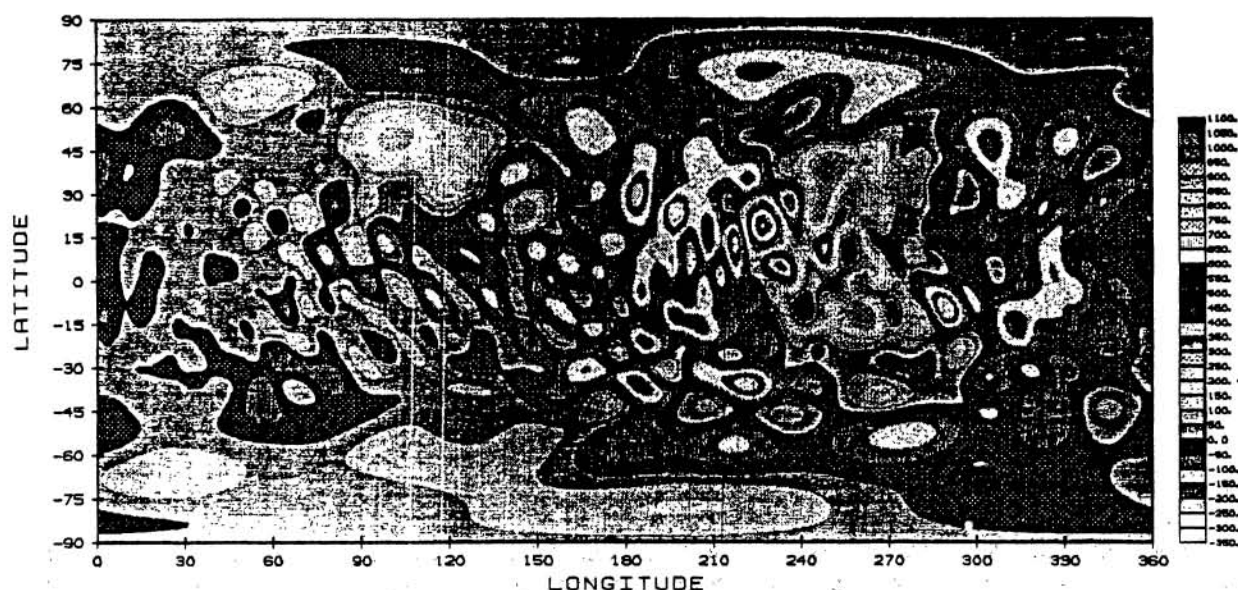


Figure 1. Free air gravity anomalies computed from Mars Gravity Model (MGM) 515 to 40x40. The contour interval is 50 mgals.